

Tunneling Rates of Single Electrons on Liquid Helium in an Extracting Field

Ismail Karakurt

Received: 4 September 2008 / Accepted: 26 November 2008 / Published online: 5 December 2008
© Springer Science+Business Media, LLC 2008

Abstract We calculated the tunneling rates of single electrons from the quasi-stationary states on both liquid ^4He and ^3He in an extracting electric field. The rates were obtained from the widths of the resonance lineshapes of the asymptotic amplitude of the wave function for the electron. The calculations were carried out in the limit of strong tunneling which leads to tunneling rates of the order of 1 GHz, and is of recent interest in a proposed quantum-computer system using the electronic states of electrons on helium as qubits. We find that the resonances can, in general, be described by Fano lineshapes. Our results, in addition to presenting quantitative information involving the read-out operations of qubits, clarify that when tunneling is weak the resonances are sharp and more accurately Lorentzian and that the observed Fano lineshapes result from strong tunneling leading to fat resonances and hence asymmetry.

Keywords Tunneling · Electrons on helium · Quantum computing · Resonance lineshapes

1 Introduction

The system of electrons on helium is among many proposed designs¹ for a quantum computer (QC). It is based on quantum bits comprised of electrons bound to a helium surface [1–7]. Each quantum bit (qubit) is made of combinations of ground and first excited states of an electron trapped over micro-electrodes just below the helium surface. Either liquid ^4He or ^3He may be used as a substrate [4, 6]. Completion of a calculation in a QC requires reading out the final states of all qubits. One of

¹ A review of concepts for quantum computers is given in Fortschritte der Physik 48(9–11) (2000) [1].

I. Karakurt (✉)

Department of Physics, Isik University, Kumbaba Mevkii, Sile, 34980, Istanbul, Turkey
e-mail: ikarakurt@isikun.edu.tr

the proposed readout schemes [4] for the proposed system above involves extracting electrons in the weakly bound excited state, $|1\rangle$, with an electric field ramp while leaving electrons in the ground state, $|0\rangle$, above micro electrodes. Then tunneling of the remaining electrons would be probed with a superconducting bolometer placed right above micro electrodes. In this proposed QC system, the times necessary for single and two-qubit operations would be ~ 1 ns and ~ 10 ns, thus the readout should be completed within the time set by single and two-qubit operations [4]. It is, therefore, crucial to know, for a readout, the strength of the external field which would yield tunneling rates on the order of 1 GHz.

In the limit of weak tunneling, i.e., for the rates smaller than 10^2 s $^{-1}$, the tunneling rates of electrons have been studied [8–14] both experimentally and theoretically. However, there have been no measurements or calculations in the limit of stronger tunneling to our knowledge. In this paper, we present numerical calculations of the single-electron tunneling rate in an extracting field which yields rates on the order of 1 GHz, on both liquid ${}^4\text{He}$ and ${}^3\text{He}$.

2 Electrons on Helium

When an electron is placed above a liquid helium surface, it is prevented from entering the liquid by an energy barrier, which is due to the Pauli force, of ~ 1.0 eV. In an externally applied field F , the Hamiltonian H , which describes the motion of the electron perpendicular to the surface, is given by

$$H = -\frac{\hbar^2}{2m} \frac{d^2}{dz^2} - \frac{Qe^2}{z} + eFz, \quad (1)$$

where $Q = (\varepsilon - \varepsilon_0)/4(\varepsilon + \varepsilon_0)$, ε is the dielectric constant of liquid helium, ε_0 is the dielectric constant of vacuum, and z is the height of the electron measured from the liquid's surface which is assumed to lie at $z = 0$. The second term in (1) is the image potential. The difference between liquid ${}^4\text{He}$ and ${}^3\text{He}$, for the problem at hand, is in their dielectric constants. Below 1 K, the ${}^4\text{He}$ and ${}^3\text{He}$ have the dielectric constants of 1.0572 and 1.0427, respectively [14].

For $F = 0$, the Schrödinger equation, $H\phi_n = E_n\phi_n$, for the electron is identical to the equation for $rR(r)$ of the zero angular momentum states of the hydrogen atom. Thus one obtains hydrogen-like solutions for the wave functions and energy eigenvalues. The ground and the first excited states, which are obtained using the usual Dirichlet boundary conditions, are given by

$$\begin{aligned} \phi_1^{\text{Hyd}}(z) &= \frac{2}{b^{3/2}}ze^{-z/b}, \\ \phi_2^{\text{Hyd}}(z) &= \frac{1}{(2b)^{3/2}}\left(2 - \frac{z}{b}\right)ze^{-z/2b}, \end{aligned} \quad (2)$$

where $b = \hbar^2/(me^2Q)$ is the effective Bohr radius. As in the hydrogen atom, the energy is quantized, and in the direction perpendicular to the surface given for an

electron on helium by

$$E_n = -\frac{R}{n^2} \quad (n = 1, 2, \dots), \quad (3)$$

where the parameter $R = \hbar^2/(2mb^2)$ is 7.6 K for ${}^4\text{He}$ and 4.3 K for ${}^3\text{He}$. This yields an energy splitting of 5.7 K (or 118.8 GHz) between the ground and the first excited states on ${}^4\text{He}$, and 4.3 K (or 67.1 GHz) on ${}^3\text{He}$.

Although the hydrogenic solutions above are qualitatively valid and describe an electron on a liquid helium surface very well for many purposes, they are not exact. The energy splitting between the ground and the first excited states, for $F = 0$, was extrapolated from the measurements [15–20] and found to be 125.9 GHz for electrons on ${}^4\text{He}$, and 69.8 GHz on ${}^3\text{He}$. The discrepancy between the hydrogenic solutions and the measurements are due to two reasons. First, the surface of the liquid helium diffuses, i.e. the liquid density drops to zero over a width [21] of about 6–7 Å at the surface, and second, the potential barrier of ~ 1.0 eV at the surface is not infinitely high. The Dirichlet boundary condition $\phi_n(0) = 0$ is, thus, inexact and the wave functions have finite amplitudes and slopes at the liquid's surface.

In order to resolve the discrepancy between the theory and the experiment, Grimes et al. [16] replaced the image potential term in H by

$$V(z) = \frac{Qe^2}{z + z_0}, \quad (4)$$

where $z_0 = 1.04$ Å. This model assumes that the image potential has its origin a distance z_0 inside the liquid. Others [21] used a smoothly varying grading function for the dielectric constant of liquid helium and the effective mass of the electron. These model calculations gave results consistent with experiments.

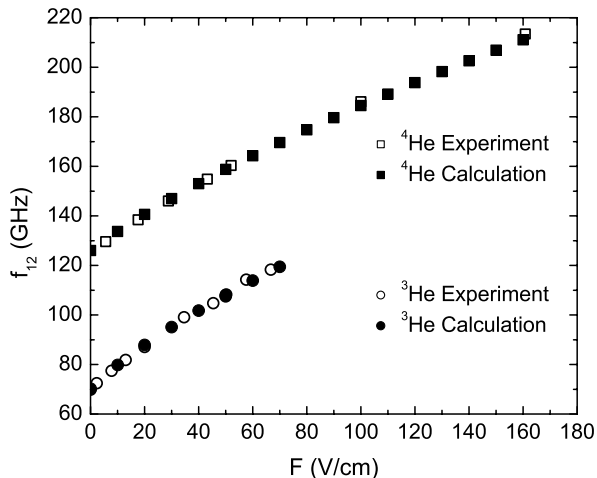
3 Numerical Calculations

In our calculations, we used Grimes' model image potential given in (4). Assuming a potential barrier of $V_0 = 1.0$ eV at the surface and an exponentially decaying solution within the liquid, the ratio of the amplitude of the wave function to its slope at the liquid's surface is approximately given by

$$\left. \frac{\phi_n}{d\phi_n/dz} \right|_{z=0} \cong \sqrt{\frac{2mV_0}{\hbar^2}} = 0.1952 \text{ nm}. \quad (5)$$

This ratio and the boundary condition that the wave functions vanish as $z \rightarrow \infty$, were used to solve the Schrödinger equation numerically in Mathematica to obtain the wave functions and the energies for an electron in the ground and the first excited states on both liquid ${}^4\text{He}$ and ${}^3\text{He}$. To test the validity of our method, we calculated the energy splitting between the ground and the first excited states for $F > 0$, and compared them with the measured values [16, 18]. In Fig. 1, we show the good agreement between our numerical calculations and the measurements.

Fig. 1 Resonant frequency f_{12} versus the applied field F for an electron on both ^4He and ^3He . The solid symbols represent the numerical calculations, while the open symbols are the experimentally measured values (by Grimes et al. [16] and Volodin and Èdel'man [18])

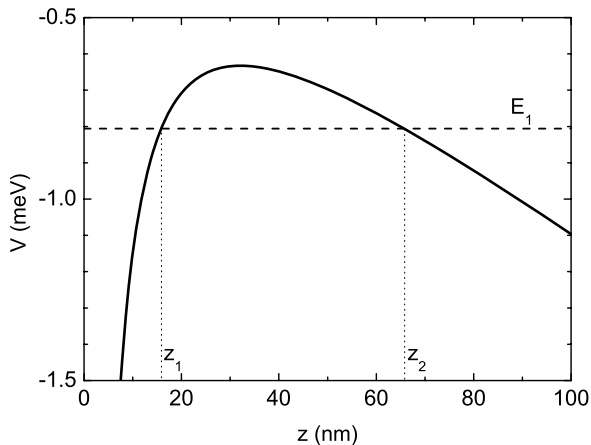


When an attractive field ($F > 0$) is applied, the wave function of the electron is squeezed resulting in a smaller effective Bohr radius, and a Stark shift between the energy levels which is clearly seen in Fig. 1. Alternatively, an extracting field ($F < 0$) has the opposite effect resulting in the escape of electrons from the surface (i.e., from the quasi-bound-states) in a time determined by the strength of the field.

Calculation of the tunneling rates of electrons involves finding the energies of the quasi-stationary states when an extracting field is applied. To obtain the energies of the quasi-stationary states for $F < 0$, the asymptotic amplitudes of the wave functions were minimized. One can look at this problem from another point of view. Consider a free electron with energy E tunneling into the potential well, defined by both the image potential $-Qe^2/(z + z_0)$ and the Stark field term $+eFz$, from outside instead of tunneling out of the well. Since the energy levels inside the well, E_n , are quantized, the amplitude of tunneling into the well will be maximum whenever $E = E_n$, i.e. at resonance. This also means that the wave function amplitude will be maximum inside the well and minimum outside of it. The resonance is also characterized by a phase change of 2π as will be shown below. We used this method to roughly estimate the quasi-bound-states energies at different electric field strengths. Similar numerical calculations were carried out by Yücel et al., in the limit of small tunneling rates ($W < 10^2$ s), to calculate the quasi-bound-state energies and lifetimes of electrons on helium from the asymptotic amplitude and phase of the wave function about the resonance energies [11, 12]. They first minimized the asymptotic amplitude to find the resonance energy, then lowered the energy until the phase decreases from its resonance value by $\pi/4$, and multiplied the reduction in energy by 2 to obtain the resonance width. Thus their lifetime calculation relied mainly on the phase data, and they did not elaborate on the dependence of the amplitude on the energy about the resonance.

Aside from being in the strong tunneling limit, our method here improves on theirs in that we were able to obtain complete lineshapes which are consistent with the phase changes in terms of the resonance widths. We find that the resonance can, in general, be characterized by a Fano lineshape.

Fig. 2 The potential energy V versus z . The dashed-line shows the energy E_1 of the quasi-stationary state obtained in the numerical calculation for an electron on ${}^4\text{He}$ at $F = -70 \text{ V/cm}$



We, now, elaborate on our method of calculation and analysis. For $F < 0$, as $z \rightarrow \infty$, the quasi-classical solution of the Schrödinger equation gives wave functions which oscillate as

$$\phi(z) \approx \frac{A}{p(z)} \sin\left(\frac{1}{\hbar} \int_{z_2}^z dz' p(z') + \delta\right), \quad (6)$$

where $p(z) = \sqrt{2m[E - V(z)]}$ is the classical momentum, z_2 is the outer turning point for the potential $V(z)$ at E (see Fig. 2), A is the asymptotic amplitude and δ is the phase shift. Both A and δ depend on energy and contain information on the quasi-stationary states' energies and lifetimes. Equation (6) is valid in the limit when

$$\alpha \equiv \left| \frac{d}{dz} \left(\frac{\lambda}{2\pi} \right) \right| \equiv \frac{\hbar m}{p^3} \left| \frac{dV}{dz} \right| \ll 1, \quad (7)$$

where $\lambda(z) = 2\pi\hbar/p(z)$ is the de Broglie wavelength of the electron. All of the data presented in this paper were obtained from the fits for which $\alpha \sim 10^{-4}$.

4 Results and Conclusions

By fitting our numerical solutions to (6) at large z , we extracted A and δ as fitting parameters as a function of energy about the resonance. To show the quality of the fits, we present the asymptotic solutions for the ground state wave function on ${}^4\text{He}$ together with their fits to (6) for $E = -0.8056 \text{ meV}$ and $E = -0.8059 \text{ meV}$ at $F = -100 \text{ V/cm}$ in Fig. 3. Note that, in the ground state, the average distance of the electron from the ${}^4\text{He}$ surface is 11.4 nm.

We should point out that the numerical calculations were carried out on a 64-bit computer, with accuracy and precision goals set between 14 and 22 figures. However, the precision of the model used is to 3 figures, e.g. due to the 3 digit precision in z_0 . We have already noted that the WKB condition is met to one part in 10^4 . In addition, we checked the effect of $\mp 1\%$ error in the parameter z_0 on the resonance energies and

Fig. 3 Numerical solutions (symbols) for the ground state on ${}^4\text{He}$ and their fits to (7) (solid lines) for $F = -100 \text{ V/cm}$. Open circles are the solution for $E = -0.8056 \text{ meV}$; and the fitting parameters are $A = 1/80.53 \text{ a.u.}$, and $\delta = 3.12 \text{ rad}$. Open squares are the solution for $E = -0.8059 \text{ meV}$; and the fitting parameters are $A = 1/101.4 \text{ a.u.}$, and $\delta = 2.48 \text{ rad}$

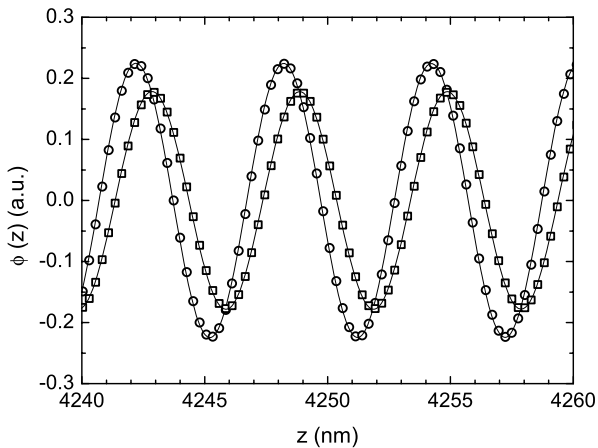
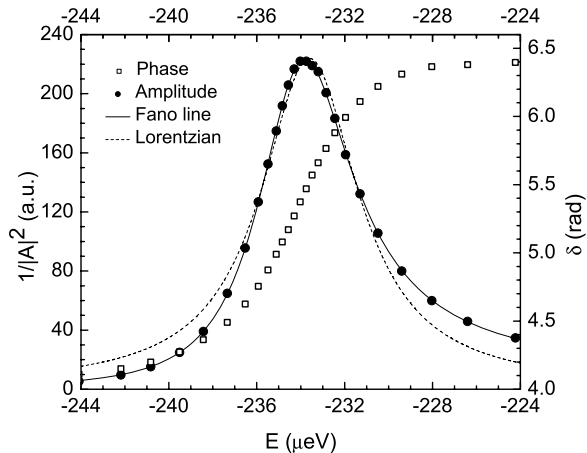


Fig. 4 The lineshape, $1/|A|^2$, of the resonance as a function of E at $F = -13 \text{ V/cm}$, for an electron in the first excited state on ${}^4\text{He}$. The solid line is a fit to the Fano lineshape (see (8)) with fitting parameters $\Gamma = 2.632 \mu\text{eV}$, $E_r = -234.2 \mu\text{eV}$, $B = 217 \text{ a.u.}$, $C = -0.132$, $D = 6.1 \text{ a.u.}$ The dotted line is a fit to a Lorentzian lineshape



tunneling rates. We find that such an error results in $\pm 0.05\%$ error in the energies, and $\mp 2\%$ error in the tunneling rates. Therefore it should be adequate to give the results in three to four significant figures.

Plots of $1/|A|^2$ and the phase δ as functions of E for the first excited state on ${}^4\text{He}$ are shown in Fig. 4 for $F = -13 \text{ V/cm}$. The center of the peak gives the energy of the quasi-stationary state. We observed that the lineshapes $1/|A|^2$ vs. E are, in general, asymmetric and do not follow the symmetric Breit Wigner form. However, they can be fitted to a Fano lineshape, which is the next simplest form, given by

$$f(E) = D + B \left[1 - \frac{(E - E_r + C\Gamma)^2}{(E - E_r)^2 + \Gamma^2} \right] \quad (8)$$

where Γ is the resonance width (half width at half maximum), E_r is the resonance energy, B is the magnitude of the resonance, C is the coefficient of the term which is responsible for the asymmetry, and D is offset. The parameter Γ/\hbar gives the tunnel-

ing rate, W , of the electron from the particular state [20]. For $C = 0$, the above Fano lineshape becomes identical with the Lorentzian.

As can be seen from Fig. 4, a Lorentzian lineshape gives a very poor best fit to the data for an electron in the first excited state on ${}^4\text{He}$ at a field of $F = -13 \text{ V/cm}$. However, it must be noted that the deviation of the lineshape from the Lorentzian disappears at small tunneling rates, i.e., as the magnitude of the applied field is reduced.

We obtained the lineshapes $1/|A|^2$ vs. E for different extracting field strengths, and obtained the tunneling rates $W = \Gamma/\hbar$ of electrons from the fits to (8). In Fig. 5, we show the tunneling rate as a function of the applied field, F , for electrons in both the ground and the first excited states on ${}^4\text{He}$. To obtain a tunneling rate of $\sim 1 \text{ GHz}$, it suffices to apply a field of $\sim (-106) \text{ V/cm}$ to an electron in the ground state. In the first excited state, a field of $\sim (-10.5) \text{ V/cm}$ yields the same rate. A comparison of

Fig. 5 Tunneling rate, W , as a function of F for electrons in the ground and the first excited states on ${}^4\text{He}$. Black squares: ground state data (bottom and left axes). Open circles: first excited state data (top and right axes). Error bars indicate the errors in the tunneling rates due to a $\sim 1\%$ uncertainty in the parameter z_0

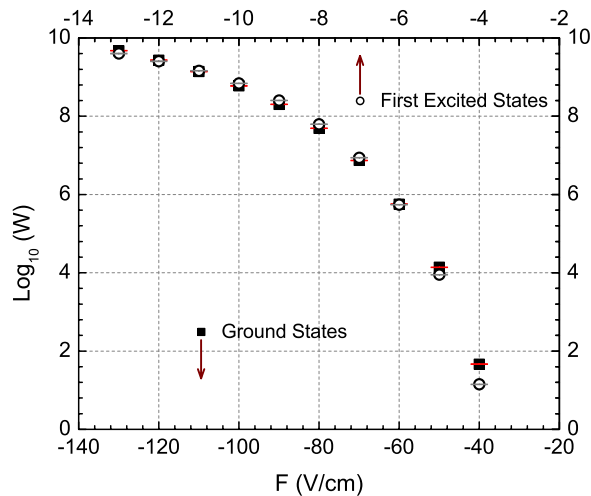
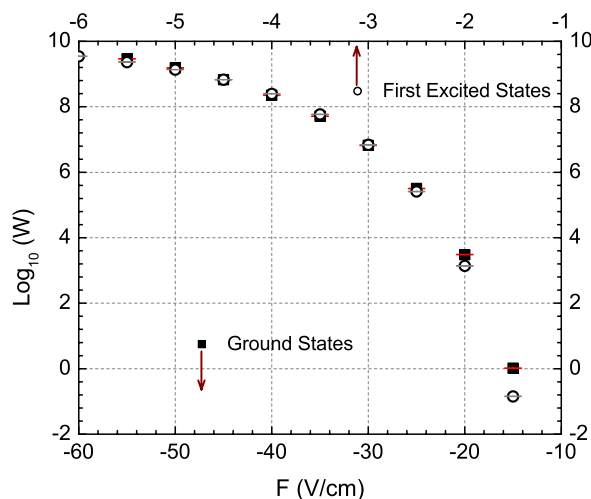


Fig. 6 Tunneling rate, W , as a function of F for electrons in the ground and the first excited states on ${}^3\text{He}$. Black squares: ground state data (bottom and left axes). Open circles: first excited state data (top and right axes). Error bars indicate the errors in the tunneling rates due to a $\sim 1\%$ uncertainty in the parameter z_0



the low tunneling rate end of our data with the results of the experiments by Saville et al. in the low electron density limit shows that our data is consistent with their measurements [13].

Similar calculations were also carried out for electrons on liquid ^3He . In Fig. 6, we show the tunneling rate as a function of F for electrons in both the ground and the first excited states on ^3He . In the case of ^3He , the fields of $\sim(-47.3)$ V/cm and $\sim(-4.70)$ V/cm yield a tunneling rate of ~ 1 GHz for an electron in the ground and the first excited states.

In conclusion, we calculated the tunneling rates of electrons from the quasi-stationary states in extracting fields on both liquid ^4He and ^3He . Calculations were carried out in the strong tunneling limit which is of recent interest in a proposed QC system using electronic states of electrons on helium as qubits. Our results present quantitative information involving the read-out operation of single qubits. Furthermore we find that the resonances can, in general, be characterized by Fano lineshapes. We clarify that when tunneling is weak the resonances are sharp and more accurately Lorentzian, and the resulting Fano lineshapes are due to strong tunneling leading to fat resonances and hence asymmetry. Our method may also be used to calculate tunneling rates and resonance lineshapes in other quasi-bound systems where the quasi-classical WKB approximation fails.

Acknowledgements The author wishes to acknowledge A.J. Dahm, H. Mathur, T. Biyikoglu and M.K. Öztürk for helpful conversations. This work was supported in part by NSF grant EIS-0085922.

References

1. M.I. Dykman, P.M. Platzman, Fortschr. Phys. **48**(9–11), 1095–1108 (2000)
2. P.M. Platzman, M.I. Dykman, Science **284**, 1967 (1999)
3. M.I. Dykman, P.M. Platzman, Fortschr. Phys. **48**, 1095 (2000)
4. A.J. Dahm, J. M Goodkind, I. Karakurt, S. Pilla, J. Low Temp. Phys. **126**, 709 (2002)
5. M.J. Lea, P.G. Frayne, Yu. Mukharshy, Fortschr. Phys. **48**, 1109 (2000)
6. A.J. Dahm, J.A. Heilman, I. Karakurt, T.J. Peshek, Physica E **18**, 169 (2003)
7. A.J. Dahm, I. Karakurt, J.A. Heilman, T.J. Peshek, Proc. SPIE **5472** (2004)
8. Y. Iye, K. Kono, K. Kajita, W. Sasaki, J. Low Temp. Phys. **38**, 293 (1980)
9. K. Kono, K. Kajita, S.-i. Kobayashi, W. Sasaki, J. Low Temp. Phys. **46**, 195 (1982)
10. J.M. Goodkind, G.F. Saville, A. Ruckenstein, Phys. Rev. B **38**, 8778 (1988)
11. S. Yücel, E.Y. Andrei, Phys. Rev. B **42**, 2088–2095 (1990)
12. E.Y. Andrei, S. Yücel, L. Menna, Phys. Rev. Lett. **67**, 3704 (1991)
13. G.F. Saville, J.M. Goodkind, P.M. Platzman, Phys. Rev. Lett. **70**, 1517 (1993)
14. H.A. Kierstead, J. Low Temp. Phys. **23**, 791 (1976)
15. C.C. Grimes, T.R. Brown, Phys. Rev. Lett. **32**, 280 (1974)
16. C.C. Grimes, T.R. Brown, M.L. Burns, C.L. Zipfel, Phys. Rev. B **13**, 140 (1976)
17. V.S. Èdel'man, Sov. Phys. JETP **50**, 338 (1979)
18. A.P. Volodin, V.S. Èdel'man, Sov. Phys. JETP **54**, 198 (1981)
19. E. Collin, W. Bailey, P. Fozooni, P.G. Frayne, P. Glasson, K. Harrabi, M.J. Lea, G. Papageorgiou, Phys. Rev. Lett. **89**(24), 245301 (2002)
20. H. Isshiki, D. Konstantinov, H. Akimoto, K. Shirahama, K. Kono, J. Phys. Soc. Jpn. **76**, 94704 (2007)
21. F. Stern, Phys. Rev. B **17**, 5009 (1978)